


 Cite this: *RSC Adv.*, 2020, 10, 37600

 Received 17th September 2020
 Accepted 6th October 2020

DOI: 10.1039/d0ra07950b

rsc.li/rsc-advances

Synthesis and modification of ZIF-8 and its application in drug delivery and tumor therapy

 Qiuxiang Wang, Yue Sun, Shangfei Li, Pingping Zhang * and Qingqiang Yao*

Metal–organic frameworks have the properties of high porosity, variable pore sizes, and easy modification as drug delivery systems. In particular, ZIF-8 based on Zn^{2+} has been extensively studied in the medical field due to its low toxicity and good biocompatibility. This review introduces the preparation and functional modification of ZIF-8, and its application in drug delivery, focusing on the single-stimulus and multi-stimulus response release of drugs in ZIF-8 materials, the integrated role of diagnosis and treatment with ZIF-8 in cancer treatment, and its application in the synergistic therapy of multiple cancer treatment methods. We summarize the latest developments of ZIF-8 in the field of drug delivery and tumor therapy, and present the main challenges that remain to be resolved in the ZIF-8 drug delivery system.

1. Introduction

Coordination polymers are compounds formed by metal ions and inorganic/organic ligands through coordination bonds. Such compounds have been widely studied due to their adjustable structure and diverse functions. A variety of related compounds were synthesized on the basis of coordination polymers, in which metal–organic frameworks (MOFs) are coordination frame materials with a porous structure formed by the coordination of metal ions or metal clusters and organic ligands. MOFs have attracted much attention due to their structural characteristics.

Compared with pure inorganic molecular sieves and porous carbon materials, MOFs have the following advantages: (1) the highly crystalline state of MOFs is very conducive in determining their precise spatial structure with single crystal and polycrystalline diffraction methods; (2) MOFs have high porosity and a specific surface area; (3) MOFs can be composed of various different metal ions and organic bridging ligands, and they have structures that are easy to design; (4) the σ single bond in the organic ligand structure gives MOFs a certain degree of flexibility, so that they have characteristic functions; and (5) the structure is easy to modify: MOFs frame and the structure of the pore surface can be adjusted by modifying the metal center and organic ligands in the MOFs framework so as to give MOFs a variety of functions.

MOFs have shown excellent performance and broad application prospects in adsorption, separation, catalysis, sensing, and drug delivery. In the field of pharmacy, MOFs have attracted much attention because of their high porosity, variable pores,

and easily modified features, which give them great application in drug delivery and sustained release.

2. Types of MOFs

Divalent metal ions (especially the first transition series), such as Mn^{2+} , Co^{2+} , Cu^{2+} and Zn^{2+} are often used to build MOFs and are used as drug carriers. According to the soft and hard acid–base theory, these metals have suitable softness and hardness, and the coordination with common donor atoms such as oxygen and nitrogen has moderate coordination reversibility. The reversibility of coordination between divalent metal ions and organic ligands gives the constructed MOFs a unique advantage in drug delivery. When the drug-loaded MOFs carrier is stimulated by a specific pH or heat, the weaker coordination bond is broken and the drug can be released. The monovalent ions such as Cu^+ , Ag^+ , and K^+ are also commonly used to construct MOFs, but they are so sensitive to light, heat, or water that the stability of the formed MOFs is usually poor, and only by using specific ligands can MOFs with a certain stability be assembled. The coordination bond formed by trivalent metal ions such as Cr^{3+} , Fe^{3+} , Al^{3+} and oxygen-containing ligands (basically carboxylic acids) has larger covalent components, and the formed MOFs often have high chemical and thermal stability. This property makes them easily react with water in the solvent during the synthesis process to form hydroxyl or oxygen-linked poly-nuclear clusters or hydroxides, which hinder the assembly and growth of MOFs. Therefore, the preparation of MOFs with Cr^{3+} , Fe^{3+} , and Al^{3+} as the center often requires acid and very high reaction temperature. Tetravalent metal ions (such as Zr^{4+}) and common oxygen-containing ligands form coordination bonds with more covalent components, and the reaction conditions are more severe.

Institute of Materia Medica, Shandong First Medical University & Shandong Academy of Medical Sciences, Jinan 250062, Shandong, China. E-mail: pingpingzhang6087@163.com; Fax: +86-0531-82919706; Tel: +86-0531-82919706





Table 1 (Contd.)

MOFs	Metal central ions	Organic ligands	Loaded drug	Applications	Reference
UiONMOF	Zr ⁴⁺	Aminotriphenyldicarboxylic acid (amino-TPDC)	Cisplatin prodrug, siRNA	Treatment of ovarian cancer	22
UiO-66	Zr ⁴⁺	BDC	Alendronate (AL)	Extra-skeletal malignancies remedy	23
UiO-66	Zr ⁴⁺	BDC	Brimonidine tartrate	Chronic glaucoma therapy	24
UiO-67	Zr ⁴⁺	4,4'-Biphenyldicarboxylic acid (BDPC)	Brimonidine tartrate	Chronic glaucoma therapy	24
Fe ₃ O ₄ @UiO-66	Zr ⁴⁺	BDC	DOX	Cure breast cancer	25
UiO-66-PNIPAM	Zr ⁴⁺	2-Amino-benzenedicarboxylic acid (H ₂ N-H ₂ BDC)	Procainamide (PROC)	Arrhythmia remedy	26

Taking into account the stability of the coordination bond between metal ions and organic ligands and the designability of organic ligands, carboxylate and pyridine ligands are often used to synthesize MOFs. The bond forming ability between carboxylate and trivalent/tetravalent metal ions is strong, and carboxylate has a negative charge, which can neutralize the positive charge of metal ions and metal clusters, so it improves the porosity and stability of MOFs. But there are many coordination modes of carboxylate, which are not easy to predict and control. The coordination mode of pyridine ligands is simple, but pyridine ligands is uncharged and their coordination ability is weak, while other components are needed to balance the positive charge of the metal ions. Carboxylate and pyridine ligands can be mixed to meet the coordination and charge requirements. In addition to the carboxylate and pyridine ligands, polyazole molecules such as imidazole and pyrazole have the advantages of carboxylate and pyridine ligands because they can remove a proton to form an anionic multi-terminal ligand. They have strong alkalinity and can form a certain intensity of coordination with metal ions, so that the synthetic MOFs have a certain stability and are widely used. MOFs synthesized from common metal central ions and different organic ligands and their applications as drug carriers are shown in the Table 1.

3. Synthesis and modification of MOFs

Commonly synthesis methods of MOF materials include the conventional solution reaction method, hydrothermal (solvothermal) method (including microwave assisted heating), diffusion method, and mechanical grinding.

The conventional solution reaction method refers to the process of directly mixing the metal salt and the organic bridging ligand in a specific solvent (such as water or organic solvent), adjusting the pH value if necessary, stirring or standing in an open system at not too high a temperature (usually below 100 °C), and precipitating the reaction products in the reaction progresses with the temperature decreases or the solvent evaporates.

The hydrothermal method or solvothermal method refers to the direct mixing of the metal salt and organic co-ligand in a specific solvent (water or organic solvent), and then putting it in a closed reactor. The reactants react under the self-generated pressure of the system through heating.

The diffusion method refers to dissolving two reactants in the same or different solvents respectively, and controlling the reaction conditions so that the two fluids containing reactants come into contact with each other through diffusion at the interface or in a specific medium, thereby reacting to form the target product.

Mechanical grinding refers to mixing and grinding the two solid phases of metal compounds and organic bridging ligand through a ball mill, and reacting to produce the target product.

Sometimes it is necessary to modify the synthesized MOFs in order to introduce some needed functional groups to give MOFs

at a much lower concentration compared with Zn^{2+} and AzA components alone.³⁴ Xing *et al.* synthesized a bio-friendly Zn-MOF $[\text{Zn}(\text{cpon})]_n$, which was constructed by semi-rigid 5-(4'-carboxyphenoxy) nicotinic acid (H_2cpon) under the guidance of the anion template strategy. $[\text{Zn}(\text{cpon})]_n$ without any tedious post-synthetic modifications, has showed the prior encapsulating behavior to 5-FU (44.75 wt%) than 6-Mercaptopurine (4.79 wt%), which indicated that the pore size of $[\text{Zn}(\text{cpon})]_n$ is more matched with 5-Fu. In addition, under a high temperature environment caused by hyperthermia, the interaction between the drug and the skeleton is destroyed, which can accelerate the drug release rate. The acidic environment will weaken the framework's restriction on 5-Fu, so the drug release speed increases with the pH decreases. Therefore, $[\text{Zn}(\text{cpon})]_n$ can be used as a drug carrier that is responsive to the thermal and pH dual-stimulus.³⁵ Yang *et al.* first synthesized a Zn-based MOF $[\text{Zn}_4\text{O}(\text{C}_8\text{H}_5\text{NO}_4)_3]$, designated as IRMOF-3 by solvothermal method, and then fabricated the folate-conjugated IRMOF-3 (FA-IRMOF-3) by conjugating the amino groups on IRMOF-3 with the carboxylic groups of folic acid. 5-FU finally loaded on the FA-IRMOF-3 to form 5-FU@FA-IRMOF-3 drug carrier particle by the impregnation method. Cytotoxicity experiments showed that folic acid as the targeting ligand on 5-FU@FA-IRMOF-3 enhanced the particle's affinity for FR-positive KB cells (human oral epidermoid carcinoma cell line) and HeLa cells (human cervical carcinoma cell line).³⁶

The zeolite imidazole framework (ZIF) is a metal-organic framework composed of Zn^{2+} and imidazole or its derivatives, which is the most widely used drug carrier in Zn-base MOFs. The most representative ZIF is ZIF-8, which is formed by the coordination of Zn^{2+} and the N atom on the 2-methylimidazole ring. Its features are as follows: high porosity, easy modification, certain thermal and chemical stability, low toxicity, and great biocompatibility. ZIF-8 is acid-sensitive and has a pH-responsive drug release function, so it has an excellent performance in drug-controlled release.

4.1 Synthesis methods of ZIF-8

4.1.1 Room temperature solution reaction method. Soltani *et al.* dissolved $\text{Zn}(\text{NO}_3)_2 \cdot 6\text{H}_2\text{O}$ in deionized water, then dissolved 2-methylimidazole in ammonium hydroxide solution, and zinc nitrate solution was added to the 2-methylimidazole solution under stirring conditions to form a gray reaction solution. The mixture became a milky suspension after 1 hour, indicating that NZIF-8 nanoparticles (NZIF-8 NPs) had been formed. The synthesized NZIF-8 NPs have a high loading capacity of gentamicin with a loading rate up to 19%. NZIF-8 NPs loaded with gentamicin can release drugs in response to pH, which is expected to treat infectious diseases caused by *Staphylococcus aureus* and *Escherichia coli*.³⁷

4.1.2 Solvothermal method. Gao added $\text{Zn}(\text{NO}_3)_2 \cdot 6\text{H}_2\text{O}$ methanol solution A to 2-methylimidazole methanol solution B under ultrasonic conditions at room temperature to make a mixed solution. The product after centrifugation of the mixed solution was ultrasonically dispersed in methanol to make solution C. Then the methanol solution of $\text{Zn}(\text{NO}_3)_2 \cdot 6\text{H}_2\text{O}$ was

mixed with solution C, and finally transferred to a 50 mL Teflon-lined stainless steel autoclave. After a solvothermal reaction at 120 °C for 2 h, the product was centrifuged and washed several times, and a hollow ZIF-8 with good crystal structure was obtained after vacuum drying.³⁸ The prepared hollow ZIF-8 possesses a high loading capacity for the anticancer drug 5-fluorouracil. The 5-fluorouracil loaded ZIF-8 material can easily be encapsulated in folic acid-chitosan-5-hydroxyfluorescein (FA-CHI-5-FAM) polymer material to give the drug cell targeting.

4.1.3 Electrodeposition-solvothermal method. Wu *et al.* firstly prepared novel ZnO/2-methylimidazole (ZnO/2-mim) nanocomposite materials with various morphologies by electrochemical deposition. Then the solid mixture of zinc chloride, 2-methylimidazole, and sodium formate was dissolved in anhydrous methanol by ultrasound, and the ZnO/2-mim nanocomposite was added. The mixed reaction solution was put into a Teflon-lined stainless-steel autoclave, and reacted for 24 hours at 85 °C under solvothermal conditions to synthesize a crack-free and uniform ZIF-8 membrane.³⁹ The ZnO/2-mim nanocomposite material provides abundant reaction sites for the synthesis of a ZIF-8 membrane which has a large specific surface area and thermal stability, and shows a high adsorption capacity for acidic drugs. It can be used for real-time dynamic monitoring of ibuprofen in patients' urine.

4.1.4 Microfluidic synthesis method. Hu *et al.* injected $\text{Zn}(\text{NO}_3)_2 \cdot 6\text{H}_2\text{O}$ methanol solution into the T-junction PDMS microfluidic reactor through inlet A with a peristaltic pump at room temperature. Then, the methanol solution containing 2-methylimidazole was stirred for 30 minutes and then divided into two equal parts, which were injected into a microfluidic reactor with a peristaltic pump through inlets B1 and B2 respectively. The product suspension was continuously collected from the outlet of the PDMS monolithic reactor, and white solid product ZIF-8 nanoparticles were obtained after centrifugation and methanol washing.⁴⁰ In the same way, ZIF-8@ SiO_2 composite nanoparticles with a uniform shape, narrow size distribution, good stability, and great biocompatibility can be continuously prepared under the condition of heating at 50 °C. The traits of strong operability and good versatility make the microfluidic synthesis method widely used in the synthesis of drugs and dye molecules loaded ZIF-8 nanocarriers.

4.2 Drug loaded methods of ZIF-8

Phenomena such as poor drug stability and non-specific targeting often occurs when therapeutic drugs are directly used, resulting in reduced drug efficacy. Increasing the amount of treatment can increase the efficacy of the drug, but it will produce greater side effects.⁴¹ ZIF-8 can be used as an intelligent drug delivery carrier to make up for the shortcomings of free drug use. There are two main strategies for loading drugs into ZIF-8: (1) the impregnation method in which drugs are loaded into the pores of MOFs through capillary force, electrostatic interaction, or coordination reaction; (2) in the growth process of MOFs, the *in situ* encapsulation of functional molecules is achieved through the one-pot method to construct drugs/MOF materials.⁴¹



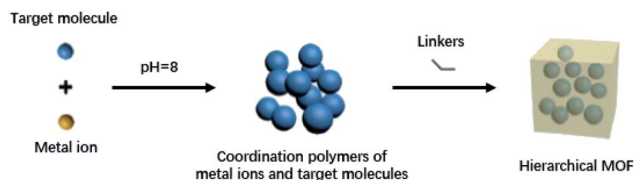


Fig. 1 pH-induced one-pot synthesis of MOF with target molecules.

4.2.1 Impregnation method. Soltani *et al.* used the impregnation method to load the antimicrobial gentamicin (GEN) into nano-ZIF-8 at room temperature to obtain gentamicin@zeolite imidazole framework nanoparticles (GEN@NZIF-8 NPs). They first dissolved GEN in methanol, then added the activated ZIF-8 powder to the GEN methanol solution, and completed the loading GEN into ZIF-8 by stirring at room temperature for 5 days. Finally, the precipitate was collected by centrifugal separation, and GEN@NZIF-8 NPs were obtained by drying after washing the precipitate with methanol.³⁷

4.2.2 One-pot method. Zheng *et al.* used a one-pot method to combine the synthesis of ZIF-8 with the anticancer drug DOX packaging process (Fig. 1). They first prepared DOX aqueous solution and 2-methylimidazole (2-mim) aqueous solution, then dissolved $\text{Zn}(\text{NO}_3)_2 \cdot 6\text{H}_2\text{O}$ in H_2O to prepare a $\text{Zn}(\text{NO}_3)_2$ solution (adjusted to $\text{pH} = 8$ by NaOH). The DOX water solution was added to the $\text{Zn}(\text{NO}_3)_2$ solution, and 2-mim solution was dropped into it after stirring for 1 minute. The reaction mixture was stirred for another 15 minutes, and the precipitate was collected by centrifugation. Finally, the precipitate was washed and dried to obtain DOX@ZIF-8.⁴² Kaur *et al.* mixed $\text{Zn}(\text{NO}_3)_2 \cdot 6\text{H}_2\text{O}$ aqueous solution, 2-methylimidazole aqueous solution, and 6-mercaptopurine (6-MP) dimethyl sulfoxide solution, which were stirred at room temperature for 5 min. Then, 6-mercaptopurine (used to treat children's acute leukemia and chronic myeloid leukemia) was loaded into ZIF-8 nanoparticles *in situ* using the one-pot method to synthesize 6-MP@ZIF-8 nanomaterials. When 6-MP is loaded into ZIF-8, the shortcomings of 6-MP's poor bioavailability and short plasma half-life are improved, and the drug treatment effect is enhanced.⁴³ Tiwari *et al.* mixed the $\text{Zn}(\text{NO}_3)_2 \cdot 6\text{H}_2\text{O}$ aqueous solution with a methanol solution of 2-methylimidazole and curcumin, which were stirred at room temperature for a certain period of time. Then a curcumin (CCM) encapsulated ZIF-8 nanomaterial (CCM-ZIF-8) was prepared by a one-pot method, and the reaction solution changed from colorless to orange, marking the successful preparation of the drug carrier. ZIF-8, as a delivery vehicle for CCM that is poorly water-soluble and rapidly degrades under physiological conditions, has a high drug load (about 83.33%), and can release drugs in response to an acidic environment.⁴⁴

4.3 Functional modification of ZIF-8

ZIF-8, a representative Zn-MOF drug delivery carrier, is stable under physiological conditions and easily degrades under acidic conditions. The polymers (such as alginate acid and polyethylene glycol) are often used to modify or decorate their surface functions to improve their stability and biocompatibility.^{45–47}

After Liu *et al.* synthesized ZIF-8 by the solution method, bis [2-(methacryloyloxy) ethyl] phosphate (BMAP) was added to the DMF solution in which ZIF-8 nanoparticles were dissolved, and a BMAP modified ZIF-8 nanoparticle solution was obtained after incubation at room temperature for 5 h. Then, azobisisobutyronitrile (AIBN) and monomers (such as acrylic acid, poly(ethylene glycol) diacrylate, and poly(ethylene glycol) methacrylate) were added to the BMAP-modified ZIF-8 nanoparticle solution, and it was incubated at 65 °C for 10 h to obtain polymer-modified ZIF-8. The polymer as a shielding layer can protect ZIF-8 from PO_4^{3-} or acid decomposition, prevent the leakage of loaded drugs, and improve the stability of ZIF-8 under physiological conditions and the stimulus-responsive release of drugs in cells.⁴⁵ Vahed *et al.* ball-milled a mixture of zinc acetate and 2-methylimidazole at room temperature to obtain ZIF-8, and then immersed ZIF-8 in the hypoglycemic drug metformin solution for drug loading. Finally, metformin loaded ZIF-8 was added to an alginate aqueous solution and alginate-modified ZIF-8 (ZIF-8@alginate) was obtained by stirring at room temperature. The surface-modified alginate of ZIF-8 increases its stability in acidic media, so that metformin loaded ZIF-8 can safely pass through the acidic media of the stomach and release the drug in the intestinal tract.⁴⁶ Wang *et al.* utilized amino poly (ethylene glycol) (PEG-NH₂) to synthesize DOX-loaded PEG-modified metal framework material DOX@ZIF-8/PEG by using a one-pot method. During the synthesis process, the particle size of ZIF-8 can be controlled by adjusting the molar ratio of PEG-NH₂ to 2-mim, and at the same time, the modification of ZIF-8 can be achieved through coordination. Pure ZIF-8 nanoparticles are easy to agglomerate. The colloidal stability of ZIF-8/PEG nanoparticles in water and cell culture fluid is greatly improved after being modified by PEG, and ZIF-8/PEG nanoparticles also have lower toxicity.⁴⁷ Surface modification often blocks the pore size of ZIF-8 and causes its drug loading to decrease. In order to solve this problem, Yan *et al.* proposed a method to synthesize an imidazole zeolite framework with controllable size and surface modification using poly-acrylate sodium salt (PAAS) nanospheres as the soft template. They first synthesized PAAS nanospheres and then mixed the nanospheres with $\text{Zn}(\text{NO}_3)_2$ methanol solution to obtain PAAS-Zn nanospheres. Then the PAAS-Zn nanospheres



Fig. 2 The process of synthesizing ZIF-8 NMOF nanocomposites using PAAS as a soft template.



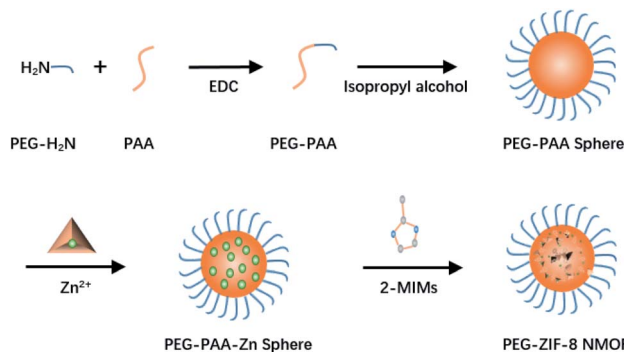


Fig. 3 The process of synthesizing PEG-modified ZIF-8 NMOF nanocomposites using PAAS as a soft template.

were dispersed in methanol, and 2-methylimidazole was added into it under stirring (Fig. 2). ZIF-8 of different sizes can be synthesized by controlling the molecular weight of PAAS, and the modified molecule can be coupled with PAAS on the surface of PAAS to achieve surface modification. This method of indirectly modifying the surface of MOFs avoids the problem of low drug loading caused by the decreased porosity of ZIF-8 after modification (Fig. 3).⁴⁸ Shearie *et al.* adopted a ball milling method to improve the hydrophobicity of ZIF-8 by using surface defect strategies. The simple ball milling method with controllable mechanical force can destroy the Zn–N bond on the surface of ZIF-8 and produce unsaturated Zn and N sites, and then the hydrophilicity of ZIF-8 is increased by bonding water molecules in a water environment. This method will not change the structure and size of the internal pores of ZIF-8, and can ensure that the hydrophilic properties of ZIF-8 are improved without affecting its drug loading capacity and release performance.⁴⁹

5. ZIF-8 composite materials

The advantages of a single metal–organic framework for drug delivery are limited. Combining ZIF-8 with other materials (such as mesoporous nanoparticles, proteins, or copolymers) to form composite materials will improve its performance, such as increasing drug loading and biocompatibility, and enhancing the sustained-release effect.

5.1 ZIF-8@Mesoporous nanoparticle composites

ZIF-8 nanoparticles are a good pH-responsive drug delivery vehicle, but the pore size of ZIF-8 nanoparticles is smaller than most drug molecules. Drug molecules are mostly adsorbed on the surface of the particles, resulting in low drug loading.⁵⁰ However, mesoporous nanoparticles (such as SiO₂, ZnO, and Fe₃O₄) often possess high drug loading efficiency due to their large specific surface area, and the controlled release of drugs can be achieved by constructing a suitable structure.^{50–52} ZIF-8 composite materials can be prepared by combining ZIF-8 with these mesoporous nanoparticles, and the synergistic effect gives them great potential in drug loading, controlled release, and monitoring.

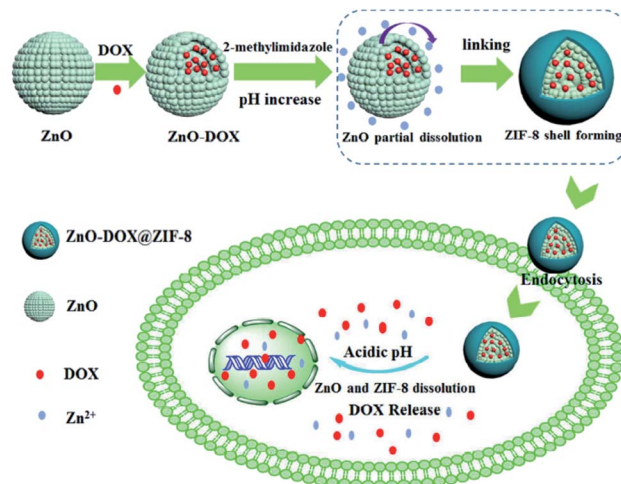


Fig. 4 Synthesis process of ZnO-DOX@ZIF-8 nanoparticles and its pH-responsive drug release mechanism.

Jia *et al.* prepared hollow mesoporous silica (HMS) by a two-step method, and then added HMS to DOX ethanol solution to synthesize DOX loaded DOX/HMS. Finally, DOX/HMS was added to the 2-methylimidazole (Hmim) and Zn(NO₃)₂ mixed solution and the DOX-loaded silica@zeolite imidazole framework (DOX/HMS@ZIF) was synthesized by stirring at room temperature. The cavity structure and radial channels of HMS are beneficial to the loading and delivery of drugs, and the weight ratio of DOX to HMS can be changed to control the drug loading of DOX. When the weight ratio of DOX to HMS is 1 : 2, the load of DOX can reach 34 wt%, and the load rate is 100%. The capsule structure constructed by DOX/HMS@ZIF encapsulates DOX in the cavity. Under physiological conditions (pH = 7.4), DOX/HMS@ZIF-8 does not release drugs, and only releases drugs at pH = 4–6. In buffer solutions of pH = 6.0, 5.0, and 4.0, the release rates of DOX/HMS@ZIF-8 within 10 h were 46.6%, 71.4%, and 85%, respectively. Compared with free DOX, the DOX/HMS@ZIF-8 drug delivery system has a longer drug release time and a better sustained release effect.⁵⁰ Zheng *et al.* used prefabricated ZnO nanoparticles as a zinc source and coordinated with 2-methylimidazole ligands to synthesize ZnO-DOX@ZIF-8 nanoparticles with a core/shell structure. ZnO in the core layer is not only a zinc source for the synthesis of MOFs, but also a core to store drugs. The pore size of ZIF-8 shell is smaller than the anti-cancer drug DOX, which protects the drug and avoids the premature release of the drug into the physiological environment. Both ZnO and ZIF-8 are unstable under acidic conditions. When ZnO-DOX@ZIF-8 is internalized by cancer cells, the ZIF-8 shell decomposes under acidic conditions, and the ZnO core is also degraded. The double decomposition of the outer shell and inner core allows the drug to be released for cancer treatment (Fig. 4).⁵¹ Cheng *et al.* synthesized Fe₃O₄ nanoparticles by the hydrothermal method, then mixed the synthesized Fe₃O₄ nanoparticles with DOX, Zn(NO₃)₂ · 6H₂O, 2-methylimidazole, and prepared DOX@Fe₃O₄-ZIF-8 nanocomposite materials by solvothermal reaction. The prepared DOX@Fe₃O₄-ZIF-8 can effectively reduce the activity of liver





Table 2 Stimulus response-controlled release of various drugs in ZIF-8 and its composites

Stimulus response type	Material	Loaded drug	The release amount in neutral environment (pH = 7.4)	The release amount in acidic environment	Application	Reference
pH	ZIF-8	5-Fu	PBS, 1 h - 17%	Acetate buffer, pH = 5.0, 1 h - 45%, 12 h - 85%	Heal colorectal, breast, head and neck cancers	2
	ZIF-8	Model drug fluorescein	PBS, 24 h - 10%	PBS, pH = 6.0, 1 h - 50%		4
	PAA@ZIF-8	DOX	PBS, 60 h - 35.6%	PBS, pH = 5.5, 60 h - 75.9%	Breast cancer cell MCF-7 treatment	54
	RGD@CPT@ZIF-8	Camptothecin (CPT)	PBS, <5%	PBS, pH = 5.0, 24 h - 75%	Cervical cancer therapy	56
	PEG-NH ₂ @As@ZIF-8	As	PBS, 24 h - 7.2%	PBS, pH = 6.0, 24 h - 20.2%	Treatment of solid tumors	58
	As@ZIF-8	As	PBS, 24 h - 15.5%	PBS, pH = 6.0, 24 h - 29.4%	Treatment of solid tumors	58
	PDA-MSN@ZIF-8	CUR + DOX	PBS, 32 h - 30% CUR + 14% DOX	Acetate buffer, pH = 5.0, 32 h - 86% CUR + 40% DOX	Breast cancer cell MCF-7 treatment	61
	ZIF-8	PHY	PBS, 72 h - 27.61%	PBS, pH = 5.0, 72 h - 88.72%; PBS, pH = 5.4, 72 h - 81.31%	Anti-microbial remedy	62
	Fe ₃ O ₄ @PAA@ZIF-8	Ciprofloxacin (CIP)	PBS, 24 h - 74%	Acetate buffer, pH = 5.0, 2 h - 20%, 3 h - 64%	Heal skin, bone, joint and respiratory infections	63
	UCNP@ZIF-8/FA	5-Fu	PBS, 12 h - 35%, 24 h - 41.5%	PBS, pH = 5.5, 12 h - 71%, 24 h - 82%	HeLa cells treatment	64
Magnetic Light	PEG-FA/PEGCG@ZIF-8	PEGCG	PBS, 48 h <15%	PBS, pH = 6.0, 10 h - 90%	Cervical cancer therapy	65
	CCM@ZIF-8/HA	CCM	PBS, 1 week - 24%	PBS, pH = 5.5, 4 days > 80%	Cervical cancer therapy	66
	HA/ α -TOS@ZIF-8	α -TOS	PBS, 25 h - no discernible release	PBS, pH = 5.0, 25 h - 74.0%	HeLa cells treatment	67
pH-redox dual stimulus	Fe ₃ O ₄ @ZIF-8	DOX	PBS, 48 h - 32.6%	PBS, pH = 5.5, 48 h - 63%	Heal breast cancer	70
	ZIF-8-TNT	DOX	PBS, the full release of DOX in the presence of UV irradiation: 25 °C - 120 min, 37 °C - 90 min		IMR-32 neuroblastoma remedy	72
pH-light dual stimulus	DOX@P/ZIF-8	DOX	PBS, in trigger of GSH agents (1 × 10 ⁻³ M), 24 h - 21.1%; in trigger of H ₂ O ₂ agents (1 × 10 ⁻³ M), 48 h - 7.0%	Acetate buffer, in trigger of GSH agents (1 × 10 ⁻³ M), pH = 5.0 24 h - 81.2%; pH = 4.2 24 h - 100%; in trigger of H ₂ O ₂ agents (1 × 10 ⁻³ M), pH = 5.0 48 h - 79.2%, pH = 4.2 6 h - 100%	Heal human breast cancer	73
	CoFe ₂ O ₄ @PDA@ZIF-8	CPT + DOX	PBS, without NIR irradiation, 40 h - 13.1% CPT, 3.2% DOX; under an 808 nm NIR laser irradiation (5 min), cumulative release 50.6% CPT, 37.2% DOX	PBS, pH = 5.0, without NIR irradiation, 61.3% CPT, 36.6% DOX; under an 808 nm NIR laser irradiation (5 min), cumulative release 74.8% CPT, 44.6% DOX	Treatment of hepatic carcinoma	75

DOX, the greater the cytotoxicity. Therefore, the anti-cancer ability of DOX@Azif-8 with different particle sizes is: 30 nm > 60 nm > 90 nm > 130 nm.⁶⁰

Stimulus-responsive drug delivery systems are receiving increasing attention because they can receive a stimulus to release a higher concentration of drugs in a specific target site while producing a smaller impact on other parts of the body. Acceptable stimuli include internal variables (pH and glutathione (GSH)) and external stimuli (light, heat, and magnetic field). The stimulus response-controlled release of various drugs in ZIF-8 and their composite materials are listed in Table 2.

6.2 Single stimulus response-controlled release of drugs

6.2.1 pH response-controlled release.

ZIF-8 can be used as pH-responsive drug release system of anti-cancer drugs, antibacterial drugs, and small molecules. The reason why ZIF-8 is pH sensitive is that acidic conditions can protonate organic ligands, leading to the cleavage of the Zn⁺-imidazolium ion coordination bond, thereby decomposing the ZIF-8 skeleton to release the drug.^{61,62}

In terms of anti-cancer drug delivery, Sun *et al.* compared the dissolution characteristics of ZIF-8 in phosphate buffer solution (PBS, pH = 7.4) and acetate buffer solution (pH = 5.0) and found that ZIF-8 dissolves fast under acidic conditions. The pH value of the tumor tissue is between 5.5–6.0, and ZIF-8 is used as the delivery carrier of 5-Fu. *In vitro* experiments showed that 5-Fu-loaded ZIF-8 has a faster drug release rate in acetate buffer, and can release more than 85% within 12 hours, which is significantly higher than its release rate in neutral solution.² Ren *et al.* used polyacrylate sodium salt nanoparticles (PAAS) as a template to synthesize PAA@ZIF-8 composite material for loading DOX. *In vitro* experiments showed that the drug release rate of the composite material can reach 75.9% after 60 h under the condition of pH = 5.5, which is much higher than its release in the medium of pH = 7.4.⁶³ Adhikari *et al.* compared the drug release rules of ZIF-7 and ZIF-8 as DOX delivery systems at pH = 7.4, 6, 5, and 4. The study found that ZIF-8 is stable under neutral conditions and easily releases drugs under acidic conditions because of the dissociation of metal ions and ligands in the framework in an acidic environment, while ZIF-7 does not release drugs under these four pH values.⁶⁴ Dong *et al.* used ZIF-8 as the carrier of the hydrophobic anticancer drug camptothecin (CPT) to synthesize CPT@ZIF-8 nanoparticles, and then mixed CPT@ZIF-8 nanoparticles with Arg-Gly-Asp (RGD) to construct a CPT-loaded RGD-modified camptothecin@zeolite imidazole framework (RGD@CPT@ZIF-8). *In vitro* drug release studies have shown that under physiological conditions (pH = 7.4), only a small amount of CPT is released (<5%), but under acidic conditions (PBS, pH = 5.0) for 24 hours, the drug release amount can reach 75%.⁶⁵ Arsenic trioxide (ATO) has not been introduced into the treatment of solid tumors due to its dose-limiting toxicity, but *in vivo* and *in vitro* studies have shown that it is a potent agent for the treatment of solid tumors. In order to improve its therapeutic effect and reduce its toxic side effects, MOFs can be used as the carrier materials.⁶⁶ Ettliger *et al.* prepared arsenic loaded As@ZIF-8 nanoparticles

and then modified their surface with amino-functionalized polyethylene glycol derivatives (PEG-NH₂) to obtain PEG-NH₂@As@ZIF-8, which can improve the biocompatibility and stability of As@ZIF-8. *In vitro* release experiments revealed that under the condition of pH = 7.4, the release amount of arsenic in As@ZIF-8 and PEG-NH₂@As@ZIF-8 after 24 h was 15.5% and 7.2%, respectively, and under the condition of pH = 6, the release of arsenic in 24 h was 29.4% and 20.2%, respectively. This shows that PEG-NH₂@As@ZIF-8 can retain the drug inside the pores under normal tissue conditions (pH = 7.4) and thus protect the environment from the drug toxic side effects, but in the more acidic microenvironment of cancer tissues, the drug can be quickly released to exert its effect. Cytotoxicity experiments show that both As@ZIF-8 and PEG-NH₂@As@ZIF-8 nanoparticles can trigger specific cytotoxicity in rhabdoid tumor cell lines at low concentrations, which is conducive to low-dose tumor treatment. The low therapeutic dose will avoid the possible toxicity of ZIF-8 to non-tumor cells (such as fibroblasts) when applied *in vivo*.⁶⁷ When chemotherapy is used to treat cancer, drug resistance is an important factor that hinders the effectiveness of drugs.⁶⁸ Combination medication is an effective way to block drug resistance.⁶⁹ Wang *et al.* synthesized a dopamine-silica@ZIF-8 (PDA-MSN@ZIF-8) core/shell structured nano-carrier to co-deliver DOX and curcumin (CUR). In the drug-loaded PDA-MSN@ZIF-8 system, the CUR-loaded ZIF-8 shell is decomposed in the acidic environment of the tumor to cause the burst release effect of CUR; then the chemotherapeutic drug DOX is continuously released from the core (PDA-MSN) to implement sequential delivery, which can effectively reduce the occurrence of drug resistance (Fig. 5).⁷⁰

In terms of antibacterial drug delivery, Soomro *et al.* loaded physcion (PHY) with anti-inflammatory and anti-microbial properties into ZIF-8 through a one-pot method at room temperature, which improved the shortcomings of low hydrophilicity and poor bio-compatibility of the drug. The release behavior of PHY@ZIF-8 in PBS (pH = 5.0, 5.4, 7.4) solution was investigated, and the results showed that the cumulative release rate of PHY under acidic conditions (pH = 5.0, 5.4) and a physiological environment (pH = 7.4) after 72 h was 88.72%, 81.31%, and 27.61%, respectively.⁷¹ Ciprofloxacin (CIP) is a fluoroquinolone antibiotic that can be used to treat skin infections, bone and joint infections, and respiratory infections. Esfahanian *et al.* synthesized Fe₃O₄@poly-acrylic acid (Fe₃O₄@PAA) particles, and then mixed them with Zn(NO₃)₂·6H₂O and 2-methylimidazole ethanol solution to prepare Fe₃O₄@PAA@ZIF-8 composite material. Finally, CIP was loaded by the impregnation method to obtain Fe₃O₄@PAA@ZIF-8@CIP drug loaded material. Studies have shown that under the condition of pH = 7.4, the drug releases about 74% after 24 hours and then remains stable, and under the condition of pH = 5, the drug release percentage after 3 hours is about 64%, which is because of the degradation of the metal-organic framework in acidic medium leads to an accelerated release rate of CIP.⁷²

In terms of small molecules delivery, due to the poor physiological stability, non-specific targeting, and low cell membrane permeability of small molecules, a higher dose is generally required to achieve the desired therapeutic effect.



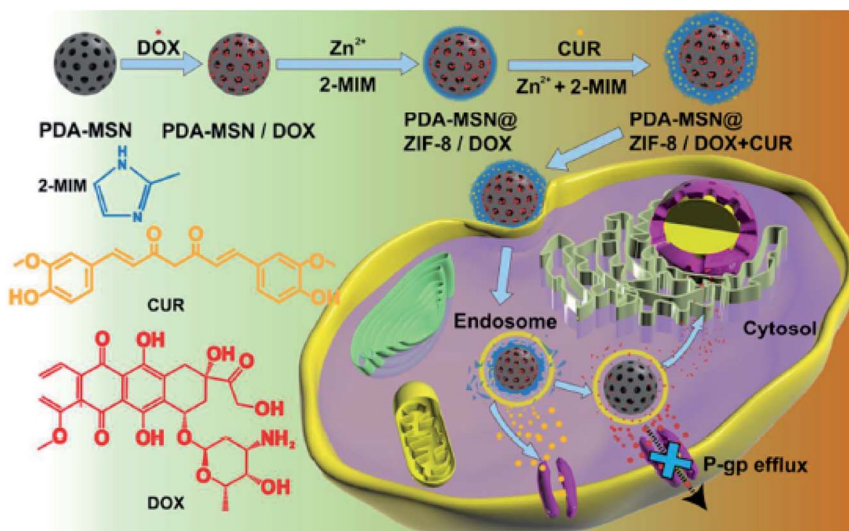


Fig. 5 The synthesis process and drug release mechanism of DOX and CUR loaded PDA-MSN@ZIF-8 core/shell nano-carriers.

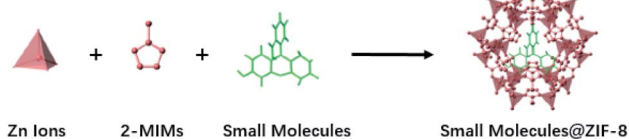


Fig. 6 The process of encapsulating small molecules into ZIF-8.

However, higher dosages will increase drug tolerance and produce adverse side effects. A more ideal therapeutic effect can be achieved by controlling the pH to regulate the release of small molecules. Zhuang *et al.* encapsulated the drug mimic fluorescein into ZIF-8 and synthesized 70 nm-sized drug-loaded nanospheres (the optimal particle size for cell uptake (<100 nm)) (Fig. 6). During the synthesis process, the concentration of fluorescein in the solution can be adjusted to reach different encapsulation amounts. The ZIF-8 nanospheres were immersed in pH = 7.4 and pH = 6.0 PBS respectively. One day later, it was found that the shape and size of the ZIF-8 nanospheres remained unchanged in the pH = 7.4 solution, while the nanospheres disintegrated in the pH = 6.0 solution. In a solution of pH = 7.4, the fluorescein release of ZIF-8 nanospheres in one day was less than 10%, and under the condition of pH = 6.0, the fluorescein release of ZIF-8 nanospheres in one hour reached 50%. This indicates that ZIF-8 can selectively release small-molecule drugs in an acidic environment, thereby realizing controlled release of drugs.⁴

6.2.2 Ligand-receptor targeted localization-controlled release. Folic acid (FA) is a simple and effective active targeting ligand. The folate receptor (FR) is an over-expressed single-chain glycoprotein, which is over-expressed in many malignant tumor cells and thus can be targeted by drug delivery vehicles with folic acid. Conjugating ZIF-8 with an active targeting ligand can deliver the drug to the target site and reduce damage to normal tissues and cells. Chowdhuri *et al.* mixed the three-

component solution containing YCl_3 , YbCl_3 , and ErCl_3 with the two-component solution of sodium hydroxide and ammonium fluoride, and synthesized $\text{NaYF}_4:\text{Yb}^{3+}$, Er^{3+} up-conversion nanoparticles (UCNPs) by the co-precipitation method. Then a core-shell structured nanoparticle (UCNP@ZIF-8/FA) based on UCNPs, MOFs, and FA was constructed by the one-pot method. Finally, the model drug 5-fluorouracil (5-FU) was loaded into it. The core-shell structured drug-loaded particles have pH response and targeted drug delivery capabilities. *In vitro* release experiments showed that after 12 h and 24 h, the release rates of 5-FU in UCNPs@ZIF-8/FA under the condition of pH = 7.4 were 35% and 41.5% respectively, while the release rates at pH = 5.5 were 71% and 82% respectively. Fluorescent microscopy studies have found that due to folate receptor-mediated endocytosis, more UCNPs@ZIF-8/FA nanoparticles are internalized by cancer cells over time, while the internalization of UCNPs@ZIF-8 nanocomposites (without FA) in cancer cells is relatively little.⁷³ Gao *et al.* synthesized hollow ZIF-8 particles by the solvothermal method, then prepared the FA-CHI-5-FAM copolymer, which was formed by the reaction between the carboxyl group of FA, 5-carboxyfluorescein (5-FAM) and the amino group of the chitosan (CHI) chain. Finally, ZIF-8 particles, the FA-CHI-5-FAM copolymer, and 5-FU were mixed under ultrasound to construct ZIF-8/5-FU@FA-CHI-5-FAM drug delivery microspheres. Among them, FA is an active targeting ligand that can target the drug to a specific location, and 5-FAM as an imaging agent can track the drug delivery process in cells in real time. The targeting of FA was evaluated by incubating ZIF-8/5-FU@FA-CHI-5-FAM and ZIF-8/5-FU@CHI-5-FAM with FA-positive MGC-803 cells and FA-negative HASMC cells respectively for 2 h. Cell uptake imaging showed that compared to ZIF-8/5-FU@CHI-5-FAM, ZIF-8/5-FU@FA-CHI-5-FAM is more easily taken up by MGC-803 cells, but almost cannot enter HASMC cells. The results demonstrated that ZIF-8/5-FU@FA-CHI-5-FAM can target the drug to the tumor site and achieve targeted sustained release of the drug.³⁸ Epigallocatechin-3-



Sharsheeva *et al.* firstly prepared TiO₂ photocatalytic nanotubes (TNTs), and then the TNTs samples were immersed in a Zn(OAc)₂·2H₂O and 2-methylimidazole solution at room temperature to obtain ZIF-8-TNT particles. Finally, DOXO was loaded into ZIF-8-TNT by the impregnation method to obtain DOXO-ZIF-8-TNT material. The *in vitro* drug release experiments showed that the time required for the complete release of drug from DOXO-ZIF-8-TNT was 41 days and 29 days when the buffer solution of pH = 7.4 was 25 °C and 37 °C, respectively, without UV light irradiation. The release process of the drug can be accelerated after lighting, and the drug can be completely released within 120 min and 90 min, respectively. Using IMR-32 neuroblastoma cells as a model, the drug release amount of DOXO-ZIF-8-TNT was about 50% after 40 minutes of ultraviolet irradiation.⁸¹

6.3 Dual stimulus response-controlled release of drugs

6.3.1 pH-redox response-controlled release. Compared with normal tissues, the tumor site is an acidic environment, and cancer cells usually express higher concentration of glutathione (GSH) or H₂O₂, so drug release can be controlled by pH and redox dual stimulation.⁸² Zhou *et al.* directly encapsulated the DOX into the ABA-type diselenide-containing triblock copolymer (PEG-PUSeSe-PEG) micelles to form DOX@P, which was mixed with 2-methylimidazole, and coordinated with Zn²⁺ to make DOX@P grow a ZIF-8 shell on the surface, and finally a core/shell structure of DOX@P/ZIF-8 drug carrier material was obtained. The *in vitro* release profiles of DOX@P/ZIF-8 under different pH conditions (pH = 7.4, 5.0, and 4.2) showed that when triggered by 1 × 10⁻³ M GSH, the protective effect of the ZIF-8 shell causes DOX@P/ZIF-8 to release only 21.1% of the

drug in 24 hours in the neutral solution, while the decomposition of the ZIF-8 shell under acidic conditions can accelerate the release of the drug, and the release of the drug in 24 h reaches 81.2% (pH = 5.0) and 100% (pH = 4.2), respectively. When triggered by 1 × 10⁻³ M H₂O₂, it also has the same pH response release trend. DOX@P/ZIF-8 also has a redox response drug release performance. In a neutral solution without GSH, DOX releases was only 5.1% after 48 hours, and the release amount in acid buffer solution is 1.6% (pH = 5.0) and 14.5% (pH = 4.2), respectively. In a solution containing a lower concentration of GSH (5 × 10⁻⁴ M), the release amount of DOX was significantly increased. In a neutral solution, the release amount was nearly 30.5% after 48 h, and the release amount in an acid buffer solution was 43.8% (pH = 5.0) and 100% (pH = 4.2), respectively. In addition, DOX@P/ZIF-8 also has a redox response to H₂O₂. The acidic condition of the tumor cause the ZIF-8 shell disintegrate, and the structure collapse of ZIF-8 lead to the breakage of the diselenium bond, which can be oxidized to selenate by H₂O₂ or reduced to selenol by GSH, causing the drug to be released from the PEG-PUSeSe-PEG micelles. This indicates that the DOX@P/ZIF-8 core/shell structure can respond to the slight redox/pH difference between tumor and normal tissues, so as to achieve the controlled-release of DOX under the dual stimulus of pH and redox.⁸² Ren *et al.* used a one-pot method to prepare DOX-loaded ZIF-8 (ZDNPs), which was used as the core. The redox-responsive silicone shell containing disulfide bonds was coated on ZDNPs to construct core-shell structured nanoparticles (ZDOS NPs), which were pH and redox dual-stimulus response. ZDOS NPs can remain stable under physiological conditions, and accumulate at the tumor site through the tumor's high permeability and retention effect

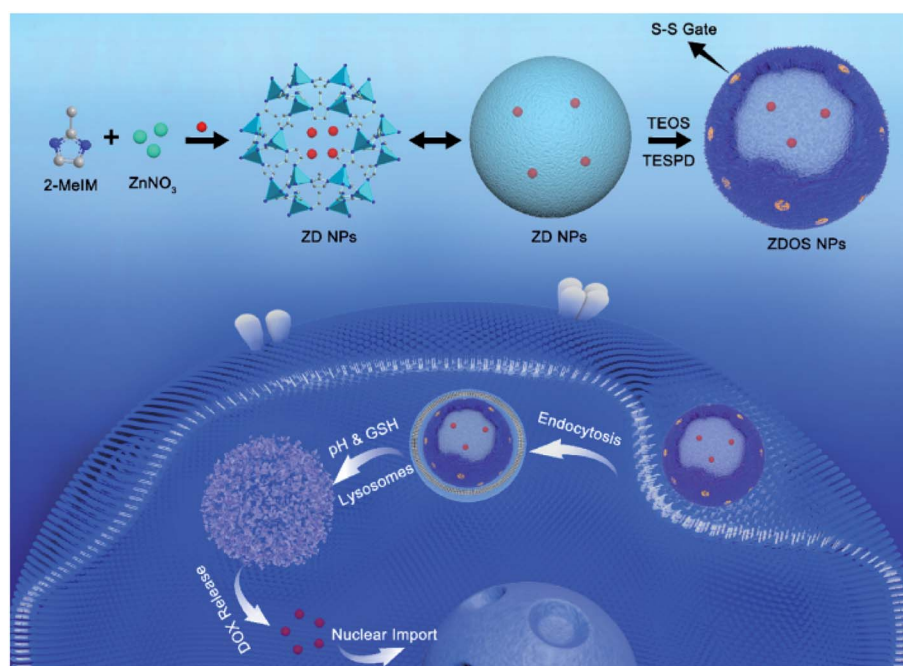


Fig. 7 The preparation and drug release process of ZIF-8@DOX@organosilicon (ZDOS) nanoparticles as a pH and redox dual response drug delivery systems.



methylimidazole (HMeIm) in isopropanol were added into it several times at 30 min intervals to obtain $\text{Fe}_3\text{O}_4\text{@PAA/AuNCs/ZIF-8}$ composite nanoparticles. Finally, DOX was loaded into $\text{Fe}_3\text{O}_4\text{@PAA/AuNCs/ZIF-8}$ by dipping. The superparamagnetism of the Fe_3O_4 core in $\text{Fe}_3\text{O}_4\text{@PAA/AuNCs/ZIF-8}$ composite material makes it is useful as a transverse relaxation (T_2) contrast agent for magnetic resonance imaging (MR). AuNCs have a higher X-ray absorption coefficient than the iodine used in conventional X-ray computed tomography (CT), which makes the CT imaging effect of composite materials better. AuNCs also has photoluminescent properties, and the fluorescent intensity of $\text{Fe}_3\text{O}_4\text{@PAA/AuNCs/ZIF-8}$ nanoparticles is 2.5 times that of discrete AuNCs, and its fluorescent imaging is better. Multi-modal imaging, which combines the three imaging technologies of MR, CT, and optical imaging, can overcome the shortcomings of single imaging. In addition, as the pH decreases, the protonation of the carboxyl group weakens the electrostatic interaction between DOX and PAA, coupled with the pH-sensitive dissolution of ZIF-8, $\text{Fe}_3\text{O}_4\text{@PAA/AuNCs/ZIF-8}$ nanoparticles have a controlled release of DOX in response to pH.⁸⁵ Shu *et al.* prepared DOX@ZIF-8 by loading the chemotherapeutic drug DOX into ZIF-8 by the one-pot method, then polydopamine (PDA) was coated on DOX@ZIF-8 by mussel heuristic polymerization to synthesize DOX@ZIF-PDA. Finally, the hyaluronic acid (HA) was coupled to DOX@ZIF-PDA through the Fe^{3+} -mediated coordination reaction to construct DOX@ZIF-8-HA material. The studies have shown that DOX@ZIF-8-HA has the ability to target prostate cancer cells (PC-3) which is overexpressed CD44. DOX can be quickly released from the carrier material in the acidic tumor environment, increasing the intracellular DOX concentration. In addition, the chelation between Fe^{3+} and PDA gives DOX@ZIF-8-HA good MR imaging capabilities.⁸⁹ Au and Ag nanomaterials are often used for surface-enhanced Raman scattering (SERS) imaging. The synergistic effect of bimetals makes the SERS performance of the Au@Ag core/shell nanorod better than that of single metal. However, when loading drugs, the shortcomings of the low specific surface area of Au and Ag limit the loading of drugs. Jiang *et al.* prepared Au nanorods (AuNRS) using a seed-mediated growth method. Then Au@Ag core/shell nanorods (Au@Ag NRS^{4-ATP}) were synthesized by the solution reaction method after mixing AuNRS, silver nitrate, and 4-aminothiophenol (4-ATP). 4-ATP gives Au@Ag NRS a strong surface Raman signal. Finally, Au@Ag NRS^{4-ATP} reacted with folic acid, $\text{Zn}(\text{Ac})_2$, and 2-methylimidazol solution to construct the Au@Ag NRS^{4-ATP}@ZIF-8/FA composite carrier. Then the impregnation method was used to load DOX into the composite carrier, which can simultaneously realize SERS imaging and

drug delivery of cancer cells. The ZIF-8 layer of Au@Ag NRS^{4-ATP}@ZIF-8/FA allows the metal nanoparticles to avoid the interference of the external environment, thereby making the Raman signal more stable.⁹⁰ The bio-imaging systems of near-infrared (NIR) persistent luminescent nanoparticles (PLNPs) can overcome the shortcomings of conventional fluorescent imaging techniques of auto-fluorescent and radiation damage. Lv *et al.* synthesized a chromium-doped zinc gallate@ZIF-8-DOX (ZGGO@ZIF-8-DOX) core/shell structure material, which had the dual functions of near-infrared persistent luminescent imaging and pH-responsive drug delivery (Fig. 8).⁹¹ Zhao *et al.* used the method of surface adsorption-induced self-assembly to grow ZIF-8 *in situ* on the surface of PLNPs ($\text{ZnGa}_{1.995}\text{Cr}_{0.005}\text{O}_4$) to prepare PLNPs@ZIF-8. PLNPs@ZIF-8 shows persistent luminescence activated by acidic tumor sites in tumor imaging. The PLNPs in PLNPs@ZIF-8 can continuously emit near-infrared light for hours or even days without external illumination, which can provide deep tissue penetration and background-free interference imaging. At the same time, the shell layer of the ZIF-8 porous framework provides good drug loading capacity, and successfully achieves drug release triggered by acidic tumor sites.⁹²

7.2 Photodynamic therapy

The rapid growth of tumor cells often causes a hypoxic micro-environment (THME) in solid tumors, and the THME will increase the malignancy and metastatic ability of tumors. Photodynamic therapy (PDT) is a method of regulating the THME to treat tumors by increasing the oxygen concentration at the tumor site. Ma *et al.* synthesized ZIF-8 nanoparticles doped with photosensitizer Chlorin e6 (Ce6) and then used the reduction effect of NaBH_4 to load nano-Au on the surface of ZIF-8 to prepare Au@ZIF-8. After Au@ZIF-8 reaches the tumor site, nano-Au with catalase-like (CAT) activity decomposes H_2O_2 to generate oxygen, and then converts the oxygen into cytotoxic reactive oxygen species under 660 nm laser irradiation to improve the efficiency of PDT, which provides a simple strategy for cancer treatment *in vivo*.⁹³

7.3 Synergistic therapy of tumor by multiple therapies

At present, the traditional treatment methods for malignant tumors mainly include surgical resection, radiotherapy, and chemotherapy, and the new treatment methods involve gene therapy, photothermal therapy, and photodynamic therapy. The complexity of tumor occurrence and development, coupled with the limitations of a single treatment make it difficult for a single treatment method to meet the treatment needs. Multi-modal

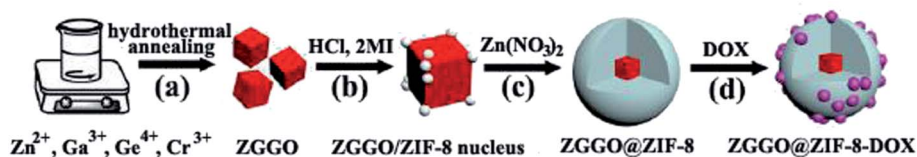


Fig. 8 Preparation of the core-shell structure ZGGO@ZIF-8-DOX multifunctional nano-platform.



- 9 B. Xiao, P. S. Wheatley, X. B. Zhao, A. J. Fletcher, S. Fox, A. G. Rossi, I. L. Megson, S. Bordiga, L. Regli, K. M. Thomas and R. E. Morris, *J. Am. Chem. Soc.*, 2007, **129**, 1203–1209.
- 10 F. Ke, Y. P. Yuan, L. G. Qiu, Y. H. Shen, A. J. Xie, J. F. Zhu, X. Y. Tian and L. D. Zhang, *J. Mater. Chem.*, 2011, **21**, 3843–3848.
- 11 P. F. Gao, L. L. Zheng, L. J. Liang, X. X. Yang, Y. F. Li and C. Z. Huang, *J. Mater. Chem. B*, 2013, **1**, 3202–3208.
- 12 D. J. Levine, T. Runcevski, M. T. Kapelewski, B. K. Keitz, J. Oktawiec, D. A. Reed, J. A. Mason, H. Z. H. Jiang, K. A. Colwell, C. M. Legendre, S. A. FitzGerald and J. R. Long, *J. Am. Chem. Soc.*, 2016, **138**, 10143–10150.
- 13 D. M. Liu, C. B. He, C. Poon and W. B. Lin, *J. Mater. Chem. B*, 2014, **2**, 8249–8255.
- 14 A. C. McKinlay, B. Xiao, D. S. Wragg, P. S. Wheatley, I. L. Megson and R. E. Morris, *J. Am. Chem. Soc.*, 2008, **130**, 10440–10444.
- 15 F. M. Wang, J. Wang, S. Z. Yang, C. Y. Gu, X. R. Wu, J. Q. Liu, H. Sakiyama, J. W. Xu, M. M. Luo and W. C. Liu, *Russ. J. Coord. Chem.*, 2017, **43**, 133–137.
- 16 P. Horcajada, C. Serre, G. Maurin, N. A. Ramsahye, F. Balas, M. Vallet-Regí, M. Sebban, F. Taulelle and G. Férey, *J. Am. Chem. Soc.*, 2008, **130**, 6774–6780.
- 17 P. Horcajada, C. Serre, M. Vallet-Regí, M. Sebban, F. Taulelle and G. Férey, *Angew. Chem., Int. Ed.*, 2006, **45**, 5974–5978.
- 18 P. Horcajada, T. Chalati, C. Serre, B. Gillet, C. Sebrie, T. Baati, J. F. Eubank, D. Heurtaux, P. Clayette, C. Kreuz, J. S. Chang, Y. K. Hwang, V. Marsaud, P. Bories, L. Cynober, S. Gil, G. Férey, P. Couvreur and R. Gref, *Nat. Mater.*, 2010, **9**, 172–178.
- 19 K. M. L. Taylor-Pashow, J. D. Rocca, Z. G. Xie, S. Tran and W. B. Lin, *J. Am. Chem. Soc.*, 2009, **131**, 14261–14263.
- 20 Y. N. Wu, M. M. Zhou, S. Li, Z. H. Li, J. Li, B. Z. Wu, G. T. Li, F. T. Li and X. H. Guan, *Small*, 2014, **10**, 2927–2936.
- 21 X. Du, R. Q. Fan, L. S. Qiang, K. Xing, H. X. Ye, X. Y. Ran, Y. Song, P. Wang and Y. L. Yang, *ACS Appl. Mater. Interfaces*, 2017, **9**, 28939–28948.
- 22 C. B. He, K. D. Lu, D. M. Liu and W. B. Lin, *J. Am. Chem. Soc.*, 2014, **136**, 5181–5184.
- 23 X. Y. Zhu, J. L. Gu, Y. Wang, B. Li, Y. S. Li, W. R. Zhao and J. L. Shi, *Chem. Commun.*, 2014, **50**, 8779–8782.
- 24 J. Gandara-Loe, I. Ortuño-Lizarán, L. Fernández-Sánchez, J. L. Alio, N. Cuenca, A. V. Estrada and J. Silvestre-Albero, *ACS Appl. Mater. Interfaces*, 2019, **11**, 1924–1931.
- 25 H. X. Zhao, Q. Zou, S. K. Sun, C. S. Yu, X. J. Zhang, R. J. Li and Y. Y. Fu, *Chem. Sci.*, 2016, **7**, 5294–5301.
- 26 S. Nagata, K. Kokado and K. Sada, *Chem. Commun.*, 2015, **51**, 8614–8617.
- 27 R. C. Huxford, J. D. Rocca and W. B. Lin, *Curr. Opin. Chem. Biol.*, 2010, **14**, 262–268.
- 28 N. Motakef-Kazemi, S. A. Shojaosadati and A. Morsali, *J. Iran. Chem. Soc.*, 2016, **13**, 1205–1212.
- 29 D. Y. Ma, J. M. Xie, Z. W. Zhu, H. L. Huang, Y. T. Chen, R. X. Su and H. M. Zhu, *Inorg. Chem. Commun.*, 2017, **86**, 128–132.
- 30 Z. D. Luo, R. Wang, C. Y. Gu, F. M. Li, Y. Y. Han, B. H. Li and J. Q. Liu, *Inorg. Chem. Commun.*, 2017, **76**, 91–94.
- 31 B. H. Song, X. Ding, Z. F. Zhang and G. F. An, *J. Iran. Chem. Soc.*, 2018, **16**, 333–340.
- 32 D. Y. Ma, Z. Li, J. X. Xiao, R. Deng, P. F. Lin, R. Q. Chen, Y. Q. Liang, H. F. Guo, B. Liu and J. Q. Liu, *Inorg. Chem.*, 2015, **54**, 6719–6726.
- 33 L. N. Duan, Q. Q. Dang, C. Y. Han and X. M. Zhang, *Dalton Trans.*, 2015, **44**, 1800–1804.
- 34 C. Tamames-Tabar, E. Imbuluzqueta, N. Guillou, C. Serre, S. R. Miller, E. Elkaïm, P. Horcajada and M. J. Blanco-Prieto, *CrystEngComm*, 2015, **17**, 456–462.
- 35 K. Xing, R. Q. Fan, F. Y. Wang, H. Nie, X. Du, S. Gai, P. Wang and Y. L. Yang, *ACS Appl. Mater. Interfaces*, 2018, **10**, 22746–22756.
- 36 B. C. Yang, M. Shen, J. Q. Liu and F. Ren, *Pharm. Res.*, 2017, **34**, 2440–2450.
- 37 B. Soltani, H. Nabipour and N. A. Nasab, *J. Inorg. Organomet. Polym. Mater.*, 2017, **28**, 1090–1097.
- 38 X. C. Gao, X. Hai, H. Baigude, W. H. Guan and Z. L. Liu, *Sci. Rep.*, 2016, **6**, 37705–37714.
- 39 M. Wu, H. L. Ye, F. Q. Zhao and B. Z. Zeng, *Sci. Rep.*, 2017, **7**, 39778–39786.
- 40 G. F. Hu, L. L. Yang, Y. N. Li and L. Y. Wang, *J. Mater. Chem. B*, 2018, **6**, 7936–7942.
- 41 X. R. Chen, R. L. Tong, Z. Q. Shi, B. Yang, H. Liu, S. P. Ding, X. Wang, Q. F. Lei, J. Wu and W. J. Fang, *ACS Appl. Mater. Interfaces*, 2018, **10**, 2328–2337.
- 42 H. Q. Zheng, Y. N. Zhang, L. F. Liu, W. Wan, P. Guo, A. M. Nyström and X. D. Zou, *J. Am. Chem. Soc.*, 2016, **138**, 962–968.
- 43 H. Kaur, G. C. Mohanta, V. Gupta, D. Kukkar and S. Tyagi, *J. Drug Deliv. Sci. Technol.*, 2017, **41**, 106–112.
- 44 A. Tiwari, A. Singh, N. Garg and J. K. Randhawa, *Sci. Rep.*, 2017, **7**, 12598–12609.
- 45 Y. Liu, C. S. Gong, Y. L. Dai, Z. Yang, G. C. Yu, Y. J. Liu, M. R. Zhang, L. S. Lin, W. Tang, Z. J. Zhou, G. Z. Zhu, J. J. Chen, O. Jacobson, D. O. Kiesewetter, Z. T. Wang and X. Y. Chen, *Biomaterials*, 2019, **218**, 119365–119375.
- 46 T. A. Vahed, M. R. Naimi-Jamal and L. Panahi, *J. Drug Deliv. Sci. Technol.*, 2019, **49**, 570–576.
- 47 H. H. Wang, T. Li, J. W. Li, W. J. Tong and C. Y. Gao, *Colloids Surf., A*, 2019, **568**, 224–230.
- 48 L. Yan, X. F. Chen, Z. G. Wang, X. J. Zhang, X. Y. Zhu, M. J. Zhou, W. Chen, L. B. Huang, V. A. L. Roy, P. K. N. Yu, G. Y. Zhu and W. J. Zhang, *ACS Appl. Mater. Interfaces*, 2017, **9**, 32990–33000.
- 49 E. Shearier, P. F. Cheng, J. M. Bao, Y. H. Hu and F. Zhao, *RSC Adv.*, 2016, **6**, 4128–4135.
- 50 X. M. Jia, Z. Y. Yang, Y. J. Wang, Y. Chen, H. T. Yuan, H. Y. Chen, X. X. Xu, X. Q. Gao, Z. Z. Liang, Y. Sun, J. R. Li, H. Q. Zheng and R. Cao, *ChemMedChem*, 2018, **13**, 400–405.
- 51 C. C. Zheng, Y. Wang, S. Z. F. Phua, W. Q. Lim and Y. L. Zhao, *ACS Biomater. Sci. Eng.*, 2017, **3**, 2223–2229.
- 52 C. Cheng, C. Li, X. L. Zhu, W. Han, J. H. Li and Y. Lv, *J. Biomater. Appl.*, 2019, **33**, 1373–1381.



- 53 Z. Z. Liang, Z. Y. Yang, H. T. Yuan, C. Wang, J. Qi, K. Q. Liu, R. Cao and H. Q. Zheng, *Dalton Trans.*, 2018, **47**, 10223–10228.
- 54 A. Ghaee, M. Karimi, M. Lotfi-Sarvestani, B. Sadatnia and V. Hoseinpour, *Mater. Sci. Eng., C*, 2019, **103**, 109767–109779.
- 55 Z. T. Lei, Q. J. Tang, Y. S. Ju, Y. H. Lin, X. W. Bai, H. P. Luo and Z. Z. Tong, *J. Biomater. Sci., Polym. Ed.*, 2020, **31**, 695–711.
- 56 X. L. Liu, Q. Yin, G. Huang and T. F. Liu, *Inorg. Chem. Commun.*, 2018, **94**, 21–26.
- 57 J. Wang, D. Y. Ma, W. L. Liao, S. J. Li, M. F. Huang, H. M. Liu, Y. F. Wang, R. Xie and J. Xu, *CrystEngComm*, 2017, **19**, 5244–5250.
- 58 M. A. Luzuriaga, C. E. Benjamin, M. W. Gaertner, H. Lee, F. C. Herbert, S. Mallick and J. J. Gassensmith, *Supramol. Chem.*, 2019, **31**, 485–490.
- 59 M. de J. Velásquez-Hernández, R. Ricco, F. Carraro, F. T. Limpoco, M. Linares-Moreau, E. Leitner, H. Wiltsche, J. Rattenberger, H. Schröttner, P. Frühwirt, E. M. Stadler, G. Gescheidt, H. Amenitsch, C. J. Doonan and P. Falcaro, *CrystEngComm*, 2019, **21**, 4538–4544.
- 60 D. B. Duan, H. Liu, M. X. Xu, M. Q. Chen, Y. X. Han, Y. X. Shi and Z. B. Liu, *ACS Appl. Mater. Interfaces*, 2018, **10**, 42165–42174.
- 61 J. Fang, Y. Yang, W. Xiao, B. W. Zheng, Y. B. Lv, X. L. Liu and J. Ding, *Nanoscale*, 2016, **8**, 3259–3263.
- 62 Z. Q. Shi, X. R. Chen, L. Zhang, S. P. Ding, X. Wang, Q. F. Lei and W. J. Fang, *Biomater. Sci.*, 2018, **6**, 2582–2590.
- 63 H. Ren, L. Y. Zhang, J. P. An, T. T. Wang, L. Li, X. Y. Si, L. He, X. T. Wu, C. G. Wang and Z. M. Su, *Chem. Commun.*, 2014, **50**, 1000–1002.
- 64 C. Adhikari, A. Das and A. Chakraborty, *Mol. Pharmaceutics*, 2015, **12**, 3158–3166.
- 65 K. Dong, Y. Zhang, L. Zhang, Z. Z. Wang, J. S. Ren and X. G. Qu, *Talanta*, 2019, **194**, 703–708.
- 66 R. Ettlinger, M. Sönksen, M. Graf, N. Moreno, D. Denysenko, D. Volkmer, K. Kerl and H. Bunzen, *J. Mater. Chem. B*, 2018, **6**, 6481–6489.
- 67 R. Ettlinger, N. Moreno, D. Volkmer, K. Kerl and H. Bunzen, *Chem.–Eur. J.*, 2019, **25**, 13189–13196.
- 68 Q. S. Pan, T. T. Chen, C. P. Nie, J. T. Yi, C. Liu, Y. L. Hu and X. Chu, *ACS Appl. Mater. Interfaces*, 2018, **10**, 33070–33077.
- 69 F. M. Zhang, H. Dong, X. Zhang, X. J. Sun, M. Liu, D. D. Yang, X. Liu and J. Z. Wei, *ACS Appl. Mater. Interfaces*, 2017, **9**, 27332–27337.
- 70 L. C. Wang, H. D. Guan, Z. Q. Wang, Y. X. Xing, J. X. Zhang and K. Y. Cai, *Mol. Pharmaceutics*, 2018, **15**, 2503–2512.
- 71 N. A. Soomro, Q. Wu, S. A. Amur, H. Liang, A. Ur Rahman, Q. P. Yuan and Y. Wei, *Colloids Surf., B*, 2019, **182**, 110364–110370.
- 72 M. Esfahanian, M. A. Ghasemzadeh and S. M. H. Razavian, *Artif. Cells, Nanomed., Biotechnol.*, 2019, **47**, 2024–2030.
- 73 A. R. Chowdhuri, D. Laha, S. Pal, P. Karmakar and S. K. Sahu, *Dalton Trans.*, 2016, **45**, 18120–18132.
- 74 X. R. Chen, Z. Q. Shi, R. L. Tong, S. P. Ding, X. Wang, J. Wu, Q. F. Lei and W. J. Fang, *ACS Biomater. Sci. Eng.*, 2018, **4**, 4183–4192.
- 75 Y. Q. Li, Y. T. Zheng, X. Y. Lai, Y. H. Chu and Y. M. Chen, *RSC Adv.*, 2018, **8**, 23623–23628.
- 76 Q. Q. Sun, H. T. Bi, Z. Wang, C. X. Li, X. W. Wang, J. T. Xu, H. Zhu, R. X. Zhao, F. He, S. L. Gai and P. P. Yang, *Biomaterials*, 2019, **223**, 119473–119483.
- 77 W. Chen, Y. Zou, F. H. Meng, R. Cheng, C. Deng, J. Feijen and Z. Y. Zhong, *Biomacromolecules*, 2014, **15**, 900–907.
- 78 K. Yang, K. Yang, S. Chao, J. Wen, Y. X. Pei and Z. C. Pei, *Chem. Commun.*, 2018, **54**, 9817–9820.
- 79 G. H. Chen, B. Yu, C. H. Lu, H. H. Zhang, Y. Q. Shen and H. L. Cong, *CrystEngComm*, 2018, **20**, 7486–7491.
- 80 J. Y. R. Silva, Y. G. Proenza, L. L. da Luz, S. de Sousa Araújo, M. A. G. Filho, S. A. Junior, T. A. Soares and R. L. Longo, *Mater. Sci. Eng., C*, 2019, **102**, 578–588.
- 81 A. Sharsheeva, V. A. Iglin, P. V. Nesterov, O. A. Kuchur, E. Garifullina, E. Hey-Hawkins, S. A. Ulasevich, E. V. Skorb, A. V. Vinogradov and M. I. Morozov, *J. Mater. Chem. B*, 2019, **7**, 6810–6821.
- 82 W. Q. Zhou, L. Wang, F. Li, W. N. Zhang, W. Huang, F. W. Huo and H. P. Xu, *Adv. Funct. Mater.*, 2017, **27**, 1605465–1605472.
- 83 S. Z. Ren, D. Zhu, X. H. Zhu, B. Wang, Y. S. Yang, W. X. Sun, X. M. Wang, P. C. Lv, Z. C. Wang and H. L. Zhu, *ACS Appl. Mater. Interfaces*, 2019, **11**, 20678–20688.
- 84 J. C. Yang, Y. Chen, Y. H. Li and X. B. Yin, *ACS Appl. Mater. Interfaces*, 2017, **9**, 22278–22288.
- 85 R. X. Bian, T. T. Wang, L. Y. Zhang, L. Li and C. G. Wang, *Biomater. Sci.*, 2015, **3**, 1270–1278.
- 86 L. He, T. T. Wang, J. P. An, X. M. Li, L. Y. Zhang, L. Li, G. Z. Li, X. T. Wu, Z. M. Su and C. G. Wang, *CrystEngComm*, 2014, **16**, 3259–3263.
- 87 Y. T. Qin, H. Peng, X. W. He, W. Y. Li and Y. K. Zhang, *ACS Appl. Mater. Interfaces*, 2019, **11**, 34268–34281.
- 88 M. N. He, J. J. Zhou, J. Chen, F. C. Zheng, D. D. Wang, R. H. Shi, Z. Guo, H. B. Wang and Q. W. Chen, *J. Mater. Chem. B*, 2015, **3**, 9033–9042.
- 89 F. P. Shu, D. J. Lv, X. L. Song, B. Huang, C. Wang, Y. Z. Yu and S. C. Zhao, *RSC Adv.*, 2018, **8**, 6581–6589.
- 90 P. C. Jiang, Y. L. Hu and G. K. Li, *Talanta*, 2019, **200**, 212–217.
- 91 Y. Lv, D. D. Ding, Y. X. Zhuang, Y. S. Feng, J. P. Shi, H. W. Zhang, T. L. Zhou, H. M. Chen and R. J. Xie, *ACS Appl. Mater. Interfaces*, 2019, **11**, 1907–1916.
- 92 H. X. Zhao, G. Shu, J. Y. Zhu, Y. Y. Fu, Z. Gu and D. Y. Yang, *Biomaterials*, 2019, **217**, 119332–119339.
- 93 Y. C. Ma, Y. H. Zhu, X. F. Tang, L. F. Hang, W. Jiang, M. Li, M. I. Khan, Y. Z. You and Y. C. Wang, *Biomater. Sci.*, 2019, **7**, 2740–2748.
- 94 Y. T. Li, J. Jin, D. W. Wang, J. W. Lv, K. Hou, Y. L. Liu, C. Y. Chen and Z. Y. Tang, *Nano Res.*, 2018, **11**, 3294–3305.
- 95 Z. F. Tian, X. X. Yao and Y. F. Zhu, *Microporous Mesoporous Mater.*, 2017, **237**, 160–167.
- 96 L. H. Su, Q. Wu, L. F. Tan, Z. B. Huang, C. H. Fu, X. L. Ren, N. Xia, Z. Z. Chen, X. Y. Ma, X. D. Lan, Q. Zhang and



- X. W. Meng, *ACS Appl. Mater. Interfaces*, 2019, **11**, 10520–10531.
- 97 H. Y. Zhang, Q. Li, R. L. Liu, X. K. Zhang, Z. H. Li and Y. X. Luan, *Adv. Funct. Mater.*, 2018, **28**, 1802830–1802839.
- 98 J. C. Yang, Y. Shang, Y. H. Li, Y. Cui and X. B. Yin, *Chem. Sci.*, 2018, **9**, 7210–7217.
- 99 L. Tang, J. F. Shi, X. L. Wang, S. H. Zhang, H. Wu, H. F. Sun and Z. Y. Jiang, *Nanotechnology*, 2017, **28**, 275601–275629.
- 100 Z. Zou, S. Q. Li, D. G. He, X. X. He, K. M. Wang, L. L. Li, X. Yang and H. F. Li, *J. Mater. Chem. B*, 2017, **5**, 2126–2132.
- 101 X. L. Wang, X. L. Li, X. Y. Liang, J. Y. Liang, C. Zhang, J. Yang, C. Wang, D. Kong and H. F. Sun, *J. Mater. Chem. B*, 2018, **6**, 1000–1010.
- 102 Q. L. Fang, Y. H. Sun, J. Y. Duan, L. F. Bai, K. Z. Xu, Q. S. Xiong, H. J. Xu, K. C. Leung, A. L. Hui and S. H. Xuan, *CrystEngComm*, 2019, **21**, 6935–6944.

